PCMI 2004 Graduate Summer School Overview

Ezra Miller and Vic Reiner

IAS/Park City Mathematics Series
Volume 00, 0000

What is geometric combinatorics?

Ezra Miller and Vic Reiner

What is geometric combinatorics? This question is a bit controversial, but at least *in part*, it is the study of **geometric** objects and their **combinatorial** structure. Rather than trying to define this precisely at the outset, in this lecture we'll mainly give examples that appear in the 2004 PCMI graduate courses.

1. Polytopes

A popular class of examples are the *convex polytopes*, that is, convex hulls of finite point sets in $\mathbb{R}^d$. These form the main topic of the graduate course by Ziegler, but also play prominent roles in the undergraduate courses by Swartz and Thomas, and in the undergraduate faculty course by Su (as well as making cameo appearances in the graduate courses by Barvinok, Fomin, Forman, MacPherson, and Wachs!).

In $\mathbb{R}^2$, convex polytopes are *polygons* such as triangles, quadrilaterals, pentagons, hexagons, etc. In $\mathbb{R}^3$ they can be more interesting, such as the triangular prism depicted in Figure 1(a).

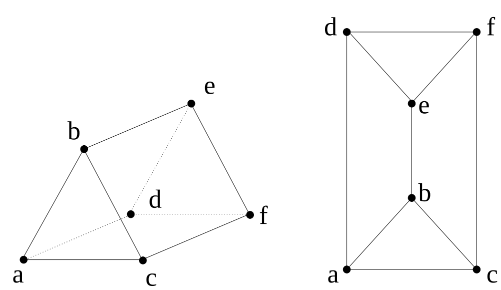

(a) (b)

Figure 1. (a) The triangular prism P, with f-vector $f(P) = (f_0, f_1, f_2) = (6, 9, 5)$. (b) Its graph or 1-skeleton, drawn as a 2-dimensional Schlegel diagram.

[1]School of Mathematics, University of Minnesota, Minneapolis MN, 55455.
E-mail address: `ezra@math.umn.edu, reiner@math.umn.edu`.

What do we mean by combinatorial structure for a convex polytope? An obvious combinatorial feature of a convex polytope is that it has *faces*, each being the intersection of the polytope with some hyperplane containing the polytope entirely in one of its two closed half-spaces. Zero-dimensional faces are called *vertices* (labelled a, b, c, d, e, f in Figure 1), one-dimensional faces are *edges*, and faces of codimension 1 within the polytope are called *facets*. One can record the combinatorial structure of the faces of a convex polytope P in varying ways and levels of detail.

- One might simply *count* the faces of various dimensions, and encode this data in the *f-vector*

$$f(P) = (f_0, f_1, \ldots, f_{d-1}),$$

  where $f_i(P)$ is the number of i-dimensional faces of P. For example, the triangular prism in Figure 1 has $f(P) = (f_0, f_1, f_2) = (6, 9, 5)$.
- One might consider the *graph* or *1-skeleton* of P; this is the abstract graph whose node set is the set of vertices of P, and whose (undirected) arcs are the edges of P. For example, Figure 1(b) depicts this graph for the triangular prism. Here we have chosen to draw this graph in the plane by projecting the whole 3-dimensional polytope P to the plane inside one of its quadrangular facets, a visualization technique known as a 2-dimensional *Schlegel diagram* for P. The back of the 2004 PCMI T-shirt depicts the 3-dimensional Schlegel diagram of a four-dimensional polytope with an interesting property, related to work of Joswig and Ziegler [**4**]: it is *dimensionally ambiguous* in the sense that this same 1-skeleton appears also for a five-dimensional polytope.
- One might further consider the entire *partially ordered set* (or *poset*, for short) of all faces of P ordered by inclusion; see Figure 2.

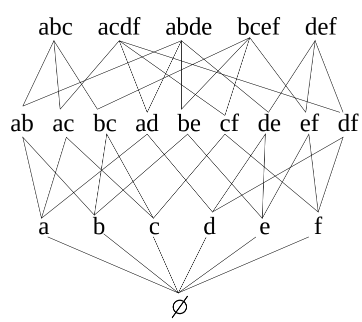

Figure 2. The *Hasse diagram* for the poset of faces of the prism in Figure 1.

2. Characterizing f-vectors

What kinds of combinatorial questions about convex polytopes might we ask? One that has been considered often is the following.

Question 1. *Which (non-negative) vectors $(f_0, f_1, \ldots, f_{d-1})$ in $\mathbb{Z}^d$ can actually arise as the f-vector of a d-dimensional convex polytope?*

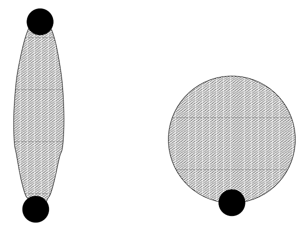

Figure 3. The digon and the monogon: two valid CW-balls, obeying the topological constraint $f_0 = f_1$. The digon has 2 vertices and 2 edges, while the monogon has 1 vertex and 1 edge.

From now on, when we speak of a "d-dimensional" polytope, we will assume that it is *fully* d-dimensional in the sense that its points affinely span a d-dimensional space. For $d = 2$, Question 1 has an obvious answer.

Proposition 2. *A vector* $(f_0, f_1) \in \mathbb{Z}^2$ *is the* f*-vector of a* 2*-dimensional convex polytope (polygon) if and only if*

(i) $f_0 = f_1$, *and*
(ii) $f_0, f_1 \geq 3$.

In spite of its simplicity, this answer foreshadows some important issues arising in higher dimensions. Note that the equation constraint (i) is really a consequence of *topology*: the boundary of a convex polygon is homeomorphic to a one-dimensional sphere. The same equation (i) would hold—without any *polytopality* assumption—for any CW-complex homeomorphic to a 2-dimensional ball, e.g. the *digon* or *monogon* depicted in Figure 3.

On the other hand, the inequality (ii) is really a consequence of polytopality. It highlights the importance of clarifying in which *category* we work when studying f-vectors (such as CW-spheres, regular CW-spheres, PL-spheres, polytopal spheres, etc.) as this can have a dramatic effect on the answers and the difficulty level for questions about f-vectors.

Question 1 for $d = 3$ is also not hard, and was answered by Steinitz roughly a century ago.

Theorem 3. *A vector* $(f_0, f_1, f_2) \in \mathbb{Z}^3$ *is the* f*-vector of a* 3*-dimensional convex polytope if and only if*

(i) $f_0 - f_1 + f_2 = 2$ *(Euler's relation),*
(ii) $f_0, f_2 \geq 4$, *and*
(iii) $2f_1 \geq 3f_2$, $2f_1 \geq 3f_0$.

Again, the equational constraint (i) is a familiar consequence of topology. Polytopality provides us with the first inequality $f_0 \geq 4$ in (ii), since we have assumed that our polytope affinely spans $\mathbb{R}^3$ and hence must have at least 4 affinely independent vertices.[2] The condition $f_2 \geq 4$ then follows from the important tool of *polar duality*: every convex polytope P in $\mathbb{R}^d$ has a (polar) dual polytope $P^\diamond$, whose faces correspond bijectively with those of P, but in an *inclusion-reversing* and *dimension-reversing* fashion. Thus for a 3-dimensional polytope P with f-vector

[2]Actually, both inequalities in (ii) already follow from (i) and (iii), and hence are redundant, but we have included them anyway.

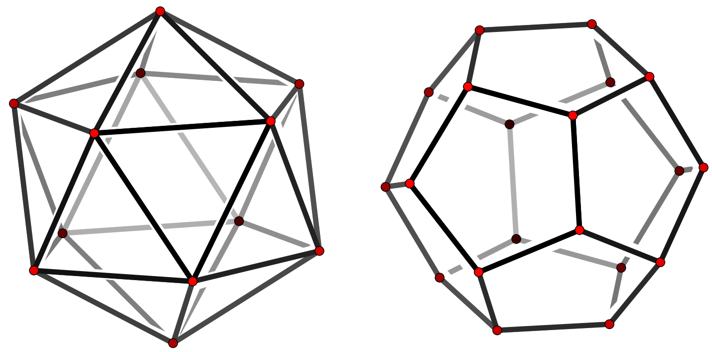

Figure 4. A pair of Platonic solids, which are polar dual to each other: the icosahedron and the dodecahedron. Their f-vectors (f_0, f_1, f_2) are related by reversal, namely $(12, 30, 20)$ and $(20, 30, 12)$, respectively.

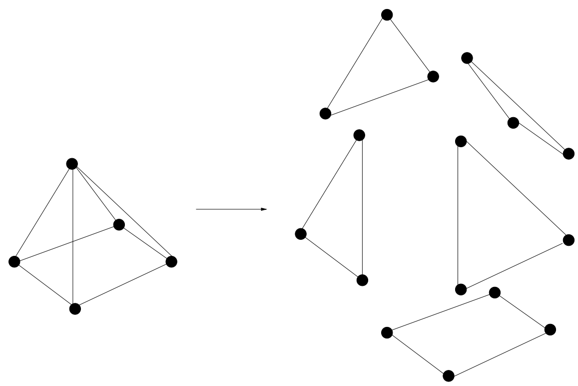

Figure 5. "Blowing apart" the facets of a 3-dimensional polytope and then counting edges in two ways shows that $2f_1 \geq 3f_2$.

(f_0, f_1, f_2), its polar dual $P^\diamond$ will have f-vector (f_2, f_1, f_0). Two classic examples of dual Platonic solids, the icosahedron and dodecahedron are shown in Figure 4.

The remaining inequalities (iii) in the above theorem are another consequence of convexity that follows from counting the edges in the polytope after "blowing apart" the facets, as depicted in Figure 5. Combining the fact that every edge lies in exactly two facets with the fact that each facet has at least three boundary edges, one is led to the inequality $2f_1 \geq 3f_2$. The second inequality in (iii) then follows from polar duality. This shows the necessity of Steinitz's conditions; the sufficiency can be shown by constructing 3-dimensional polytopes with specified f-vectors via some relatively simple constructions (start with a pyramid having an arbitrary polygonal base, and iterate the operation of *shaving off* a vertex, or its polar dual operation of *stellarly subdividing* a facet).

What about Question 1 for $d \geq 4$? In dimension 4 there are only partial answers (see Ziegler's course), and in higher dimensions, the question is wide open.

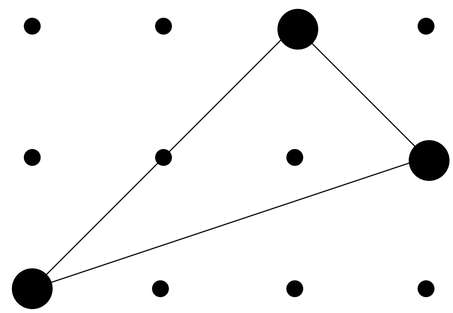

Figure 6. The area of a lattice triangle having $i = 1$ interior lattice point and $b = 4$ boundary lattice points is $i + \frac{1}{2}b - 1 = 2$.

3. Lattice points

There is even more combinatorial structure attached to *lattice polytopes*, the topic of the graduate course by Barvinok, appearing also in the undergraduate course by Thomas as well as the undergraduate faculty course by Su. A lattice polytope is a convex polytope whose vertices lie in $\mathbb{Z}^d$. Here there are non-trivial results even for $d = 2$, that is for lattice polygons! The most famous is probably *Pick's formula* for the area of a lattice polygon.

Theorem 4. *(Pick [**6**]) Let P be a lattice polygon with i lattice points in its interior and b lattice points on its boundary. Then the area of P is $i + \frac{1}{2}b - 1$.*

Figure 6 illustrates this result for a certain lattice triangle. In fact, Pick's Theorem holds even for lattice polygons which are not convex.

The theory of lattice polytopes becomes more interesting in higher dimensions, including the theory of *Ehrhart polynomials.* It is a subject that has seen many advances within the last decade that have greatly increased our ability for explicit computations. One such advance is *Brion's formula*, which says how to list the lattice points in a lattice polytope. More precisely, let P be a polytope in $\mathbb{R}^d$ with integer vertices. If $\mathbf{a} = (a_1, \ldots, a_d) \in \mathbb{Z}^d$ is a lattice point, then write $\mathbf{t}^{\mathbf{a}} = t_1^{a_1} \cdots t_d^{a_d}$ for the corresponding Laurent monomial. The generating function for the lattice points in P is the sum of all Laurent monomials $\mathbf{t}^{\mathbf{a}}$ for $\mathbf{a} \in \mathbb{Z}^d \cap P$. It is a rational function because it has only finitely many terms. In contrast, consider the *tangent cone* $T_{\mathbf{v}}$ to the polytope at the vertex $\mathbf{v}$, which is the translate by $\mathbf{v}$ of cone generated over the positive real numbers by $P - \mathbf{v}$. The generating function for the lattice points $\mathbb{Z}^d \cap T_{\mathbf{v}}$ in a tangent cone is not a finite sum, but it is still expressible as a rational function $C_{\mathbf{v}}(\mathbf{t})$. Brion's formula breaks the lattice point enumerator of P into a sum over the vertices of P:

$$\sum_{\mathbf{a} \in \mathbb{Z}^d \cap P} \mathbf{t}^{\mathbf{a}} = \sum_{\text{vertices } \mathbf{v} \text{ of } P} C_{\mathbf{v}}(t).$$

This counter-intuitive result looks like it counts each lattice point in P once for each vertex of P, and furthermore counts all of the lattice points outside of P some number of times, as well. But when that wild-looking generating function (supported on all of $\mathbb{Z}^d$) is expressed as a single rational function, the over-counting inside of P and parts outside of P vanish. Brion's formula is important for computation because it provides a "short" way to represent the set of lattice points in P.

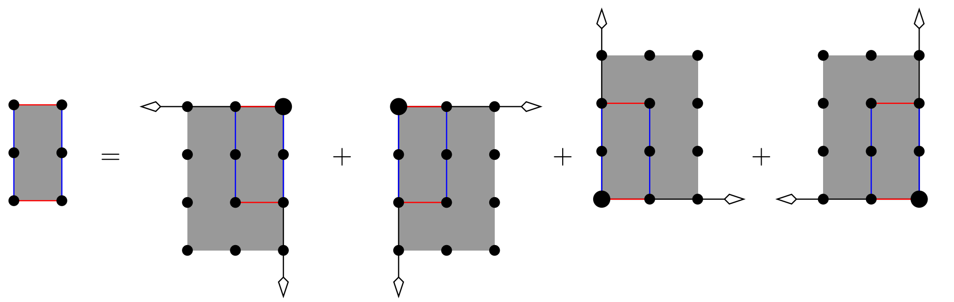

$$\begin{aligned}
&= \frac{st^2}{(1-s^{-1})(1-t^{-1})} + \frac{t^2}{(1-s)(1-t^{-1})} + \frac{1}{(1-s)(1-t)} + \frac{s}{(1-s^{-1})(1-t)} \\
&= \frac{s^2t^3 - t^3 + 1 - s^2}{(1-s)(1-t)} \\
&= \frac{(1-t^3)(1-s^2)}{(1-s)(1-t)} \\
&= (1+t+t^2)(1+s) \\
&= 1 + t + t^2 + s + st + st^2
\end{aligned}$$

Figure 7. Brion's formula verified for the 2×1 lattice rectangle in $\mathbb{R}^2$

Example 5. Let $P \subset \mathbb{R}^2$ be the 2×1 lattice rectangle

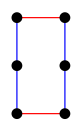

with vertex set $\{(0,0),(1,0),(2,0),(1,2)\}$. The lattice point enumerator of P, written in variables $(s,t) = (t_1,t_2)$, is $1 + t + t^2 + s + st + st^2$. The lattice points in the tangent cone at (say) the vertex $(1,2)$ of P consist of all integer vectors (a,b) such that $a \leq 1$ and $b \leq 2$. The generating function for these lattice points is $st^2/(1-s^{-1})(1-t^{-1})$. The statement of Brion's formula in this case is verified in the calculation appearing in Figure 7.

4. Hyperplane arrangements

Another interesting example of geometric objects with combinatorial structure are arrangements of *hyperplanes*, the subject of Stanley's graduate course, and other (affine or) linear subspaces of a vector space, which form part of the subject of Wachs's graduate course. Figure 8 illustrates an affine arrangement of hyperplanes (lines) in $\mathbb{R}^2$, along with a *central* arrangement of hyperplanes in $\mathbb{R}^3$ depicted via their intersections with the unit sphere.

Hyperplanes dissect $\mathbb{R}^d$ into open *regions* (or *chambers*), which can be bounded or unbounded, and which one can attempt to count. When one complexifies real hyperplanes or subspaces by considering them inside $\mathbb{C}^d$, they "poke holes" in the space, creating non-trivial topology one can try to measure, e.g. by computing homotopy invariants such as homology or homotopy groups, or cohomology rings. When the hyperplanes or subspaces are defined over $\mathbb{Z}$, one can consider their

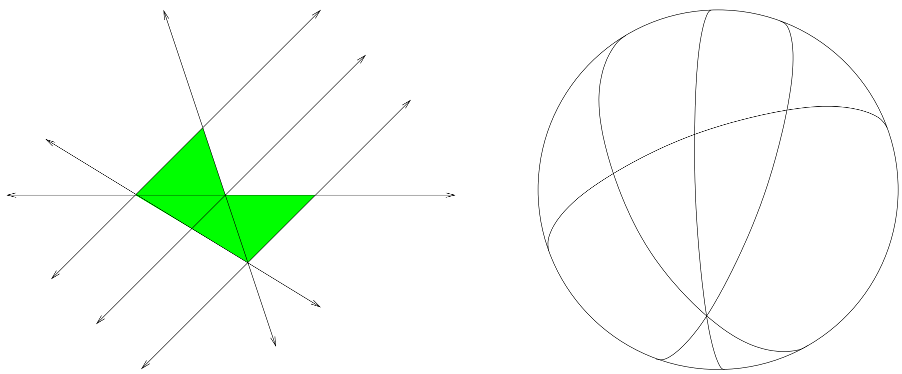

Figure 8. An arrangement of affine lines in $\mathbb{R}^2$ with the bounded regions shaded, and a central arrangement of hyperplanes in $\mathbb{R}^3$ depicted as great circles on a unit sphere.

reductions mod p as arrangements in vector spaces $\mathbb{F}_p^d$ over finite fields, and then count points lying on or off the arrangement. It turns out that almost all of this enumerative or topological analysis comes down to understanding the *topology* of another poset: the *lattice of intersections* of the subspaces, ordered by inclusion.

In particular, one learns that it is important to associate a simplicial complex (and hence a topological space) to this poset, via the ubiquitous *order complex* or *nerve* construction. We also find ourselves in need of a wide array of tools, provided in the graduate course on poset topology by Wachs, for understanding the homotopy or homeomorphism type of the various kinds of simplicial complexes that arise in this way.

5. Symmetry

Many of the examples of combinatorial geometric objects cropping up all over mathematics, such as in the geometry and representation theory of Lie groups and algebras, are those possessing a high degree of *symmetry.* Such objects are the subject of the graduate course by Fomin, and also play a prominent role in the part of Wachs's course that deals with the *equivariant theory* of poset topology.

To give some flavor of Fomin's course, let's look briefly at the classical topic of *regular polytopes.* A regular polytope is one in which every *maximal flag* of faces

$$\text{vertex} \subset \text{ edge} \subset \cdots \subset \text{ facet}$$

"looks" the same, meaning that the group of linear symmetries preserving the polytope acts transitively on all such flags. The 3-dimensional regular polytopes are exactly the Platonic solids, depicted in Figure 4. Classical results in the theory associate to every regular polytope P a certain well-studied and well-behaved hyperplane arrangement: the symmetry group of a regular polytope is always generated by *reflection symmetries*, and one simply takes the associated reflecting hyperplanes for all such symmetries. For the regular tetrahedron, the associated dissection by reflecting hyperplanes and the hyperplane arrangement are shown in Figure 9. Not only do these reflection arrangements play a central role in Fomin's course, but they show up as key motivating examples, along with some of their well-behaved deformations, in Stanley's course as well.

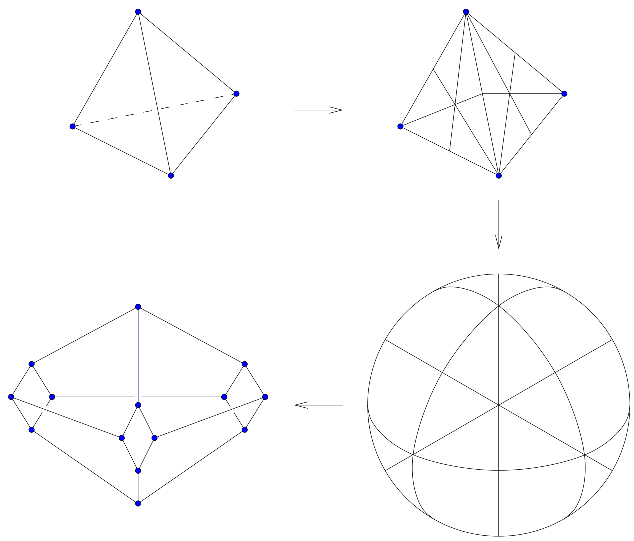

Figure 9. The reflection symmetries of the regular tetrahedron, dissecting its boundary. The associated reflection hyperplane arrangement and root system gives rise to the 3-dimensional associahedron, with f-vector $(f_0, f_1, f_2) = (14, 21, 9)$. Note that $f_0 = 14 = \frac{1}{5}\binom{2\cdot 4}{4} = C_4$ is a Catalan number.

A collection of vectors consisting of a pair of two opposite normal vectors for each of these reflecting hyperplanes gives rise to what is called a *root system*. It should be noted that not every root system comes from the reflection arrangement of a regular polytope, but three of the four infinite families of (finite, irreducible, crystallographic) root systems (types A, B, and C) do arise in this way from the higher-dimensional regular polytopes that generalize tetrahedra (simplices) and cubes/octahedra (hypercubes/hyperoctahedra).

Moving beyond the classical theory, an exciting development in 21st century geometric combinatorics (and a main focus of Fomin's graduate course) has been the discovery of what are called *cluster algebras*. The cluster algebras of finite type give rise to new and important convex polytopes associated to root systems, called *generalized associahedra*. For root systems of type A, these are the classical *associahedra* or *Stasheff polytopes* which have been known for decades in topology, geometry and algebra. The bottom part of Figure 9 depicts the type A associahedron arising from the reflection arrangement for the regular tetrahedron. In type B, one recovers the more recently discovered *cyclohedra* of Bott and Taubes.

These polytopes exhibit wondrous numerology, closely connected with *Catalan numbers* $C_n = \frac{1}{n+1}\binom{2n}{n}$ in type A, and more generally with the mysterious numerology of *exponents* for all root systems. A great deal of intriguing combinatorics awaits discovery in these polytopes.

6. Moment graphs

Geometric combinatorics does not only concern structures arising from spaces that feel discrete. Smooth spaces often have underlying combinatorics, as well. Many smooth spaces can be considered from the point of view in MacPherson's course,

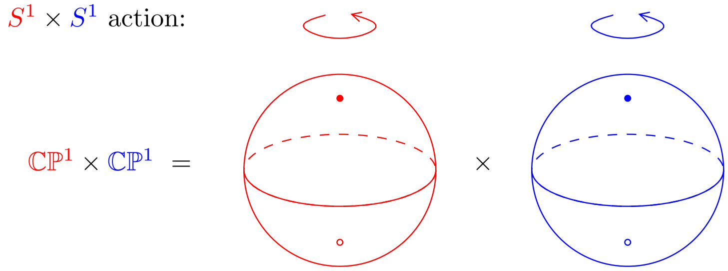

Figure 10. $\mathbb{CP}^1 \times \mathbb{CP}^1$ and the action of $S^1 \times S^1$

where the combinatorics takes the form of a graph drawn with straight edges in $\mathbb{R}^n$. The setup is as follows.

An *algebraic torus* is a group of the form $T = (\mathbb{C}^*)^n$, where $\mathbb{C}^* = \mathbb{C} \setminus \{0\}$ is the set of nonzero complex numbers, considered as a group under multiplication. Inside of the algebraic torus T is an honest compact torus $T_\mathbb{R} = (S^1)^n$, the product of n copies of the unit circle group. MacPherson's course concerns spaces X with an action of T. More precisely, let X be a smooth compact complex algebraic variety of dimension d; thus X is a real manifold of dimension $2d$ with some extra structure to make it a manifold over $\mathbb{C}$. We require that the action $T : X \to X$ has finitely many

- T-fixed points and
- complex 1-dimensional orbits.

An orbit of complex dimension 1 has real dimension 2, and is necessarily isomorphic to a copy of $\mathbb{C}^*$. Since X is compact, the closure of such an orbit is an isomorphic copy of the Riemann sphere (projective complex line) $\mathbb{P}^1$: add an origin 0 and a point ∞ at infinity (both of which will be T-fixed points) to the copy of $\mathbb{C}^*$. The union of the T-fixed points and the 1-dimensional orbits is a configuration, called a *balloon sculpture*, of finitely many Riemann spheres in X joined at some of their poles. The *moment graph* is a real 1-dimensional shadow of the complex 1-dimensional balloon sculpture. It is obtained from the balloon sculpture by identifying together all points in each orbit of the compact torus $T_\mathbb{R}$.

Example 6. Let $X = \mathbb{CP}^1 \times \mathbb{CP}^1$ be a product of two Riemann spheres. This space comes with an action of $T = \mathbb{C}^* \times \mathbb{C}^*$, so $n = 2$ in the preceding notation. The compact torus $T_\mathbb{R} = S^1 \times S^1$ is the familiar real 2-dimensional doughnut. The two copies of S^1 spin the corresponding spheres $\mathbb{CP}^1$ around their axes, each leaving the other sphere fixed pointwise, as depicted in Figure 10. The balloon sculpture in X consists of four spheres joined pole-to-pole in a cycle, as in Figure 11. The circles of latitude in the four balloons are $T_\mathbb{R}$ orbits, as are each of the poles. Collapsing each of these orbits to a point yields the moment graph of $\mathbb{CP}^1 \times \mathbb{CP}^1$: a square.

In the above example, the quotient of all of X by $T_\mathbb{R}$ is the entire square—including the interior, over which the $T_\mathbb{R}$ orbits are 2-dimensional tori. More generally, for every lattice polytope P there is a *toric variety* X_P whose moment graph is the edge graph of P, and whose quotient by $T_\mathbb{R}$ is all of P. Although toric varieties constitute a very important class of examples—they are the simplest spaces with moment graphs—they aren't the only spaces with moment graphs.

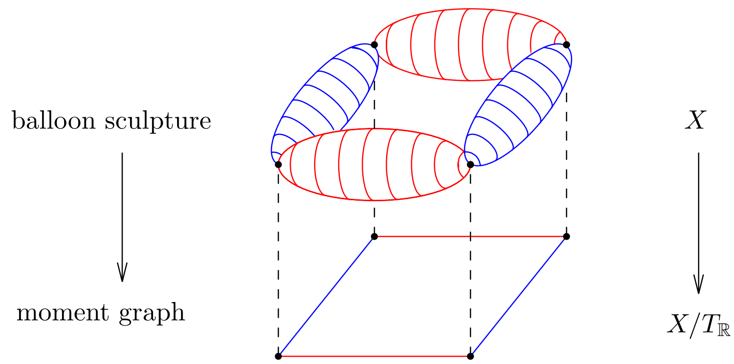

Figure 11. The balloon sculpture of $X = \mathbb{CP}^1 \times \mathbb{CP}^1$ and its map to the moment graph

Example 7. Let X be the quadric hypersurface in $\mathbb{CP}^6$ consisting of the solutions to the polynomial equation $z^2 + x_1y_1 + x_2y_2 + x_3y_3 = 0$. The algebraic torus $T = (\mathbb{C}^*)^3$, with coordinates (τ_1, τ_2, τ_3), acts by

$$(\tau_1, \tau_2, \tau_3) \cdot (z : x_1 : x_2 : x_3 : y_1 : y_2 : y_3) = (z : \tau_1 x_1 : \tau_2 x_2 : \tau_3 x_3 : \tau_1^{-1} y_1 : \tau_2^{-1} y_2 : \tau_3^{-1} y_3);$$

that is, the polynomial equation is invariant under T. The moment graph is ubiquitous when it comes to this summer school. In particular, there is geometric combinatorics on the front of the 2004 PCMI T-shirt as well as on the back! This example is straight from MacPherson's notes, where it is treated in more detail.

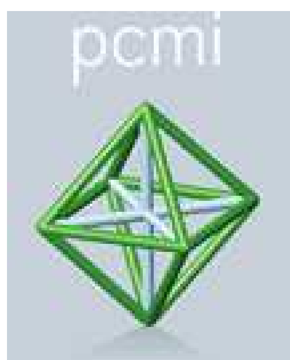

Figure 12. The moment graph of the quadric hypersurface X in $\mathbb{CP}^6$

The methods surrounding moment graphs are particularly well-suited to spaces like complete flag manifolds and their relatives, including Grassmannians, other quotients of compact Lie groups by parabolic subgroups, and loop Grassmannians. These spaces are crucial to interactions of combinatorics with representation theory and algebraic geometry. Moment graphs (and *moment maps*, when they are available) are vehicles by which smooth spaces give rise to more obviously discrete-geometric objects such as polytopes, graphs, and root systems. A hint of the consequences of this transition occurs in Fomin's graduate course.

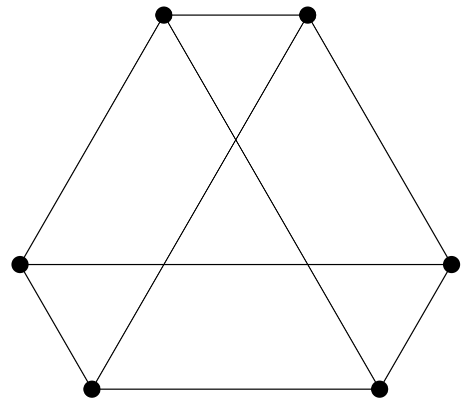

Figure 13. The convex hull of the moment graph of the flag manifold $\mathcal{F}\ell_3$ is a permutohedron

Example 8. Let $X = \mathcal{F}\ell_3$ be the manifold of flags in $\mathbb{C}^3$. Thus $\mathcal{F}\ell_3$ consists of the chains $\{0\} = V_0 \subset V_1 \subset V_2 \subset V_3 = \mathbb{C}^3$ of vector subspaces of $\mathbb{C}^3$ with $\dim V_i = i$. The algebraic torus $(\mathbb{C}^*)^3$ naturally acts on X by virtue of its action on $\mathbb{C}^3$. The moment graph of $\mathcal{F}\ell_3$ is depicted in Figure 13. The graph can be naturally embedded in a plane sitting in $\mathbb{R}^3$, and its convex hull, which is the image of the moment map, is a hexagon. More generally, the convex hull of the moment graph of the manifold $\mathcal{F}\ell_n$ of flags in $\mathbb{C}^n$ is a polytope called the *permutohedron*, whose vertices are the $n!$ permutations of $(1, \ldots, n)$. Unlike the moment graphs of toric varieties (but like the PCMI logo in Figure 12), the edges of the permutohedron constitute only part of the moment graph of $\mathcal{F}\ell_n$, which also has edges passing through the interior.

7. Fixed points of smooth symmetries

Moment graphs isolate combinatorial structures from a priori smooth geometric contexts. But what is this combinatorial data good for? Although it may not seem likely at first, the moment graph actually retains an enormous amount of information about a space X. In particular, much of the topology of X can be faithfully recovered from the discrete data of its moment graph.

This sort of claim reflects a phenomenon that is quite general. Without introducing too many hypotheses, the setup is that X should be a space with an action of some Lie group G such that the set X^G of fixed points is finite. Now suppose that ξ is some global topological invariant of X that is *G-equivariant*, meaning that it takes into account the G-action. The aim is to produce statements saying that

$$\xi = \sum_{x \in X^G} \xi_x$$

breaks up as a sum of local contributions ξ_x at the fixed points. Theorems of this form are called *localization theorems* or *fixed point formulas*, and often come attached to names such as Atiyah, Bott, or Lefschetz. The idea is that the residual action of G on the tangent spaces to the G-fixed points carries enough information about the action on X to reconstruct topological data.

In MacPherson's course, ξ is an equivariant cohomology class or some related invariant, the point being that the entire equivariant cohomology ring of X is determined by its moment graph. In Barvinok's course, taking ξ to be the character of the global sections of a line bundle on a toric variety yields Brion's theorem as a statement in equivariant K-theory. For instance, the computation in Example 5 comes from localization applied to the line bundle $\mathcal{O}(1,2)$ on the toric variety from Example 6. Of course, this key to Barvinok's polynomial-time algorithms for lattice point enumeration does not, in a logical sense, require thinking about equivariant K-theory of toric varieties; but it is worthwhile to note that it was in such a context that Brion discovered the formula in the first place.

The notion that topology is encoded by local data near fixed points is a powerful one. Even forgetting temporarily about the two preceding examples, it has far-reaching consequences, combinatorial and otherwise, ranging from Okounkov and Pandharipande's proof of Witten's conjecture (Kontsevich's theorem) [**5**] to Deligne's proof of the Weil conjectures (see [**2**]).

Yet another example underlies a fundamental part of the geometry in Haiman's course. The smooth space there is the *Hilbert scheme* H_n of n points in the plane $\mathbb{C}^2$. As a set, H_n consists of the ideals $I \subseteq \mathbb{C}[x,y]$ in the two-variable polynomial ring such that $\mathbb{C}[x,y]/I$ has dimension n as a vector space over $\mathbb{C}$. The ideal of polynomials vanishing on n distinct points in $\mathbb{C}^2$ is an example of a point $I \in H_n$. However, there are other colength n ideals, such as the ideal generated by x^n and y; a $\mathbb{C}$-linear basis for the quotient $\mathbb{C}[x,y]/I$ is given by $\{1, x, x^2, \ldots, x^{n-1}\}$.

More generally, for every *partition* λ of n, meaning a weakly decreasing list of integers whose sum is n, there is an ideal I_λ generated by monomials. Think of λ as a (Young) shape, so that for example

$\lambda = (7,4,2,2,1) \quad \longleftrightarrow$

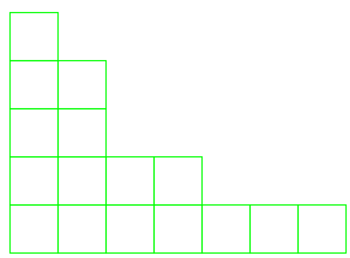

is a partition of $7+4+2+2+1 = 16$ in "French" notation. The nooks immediately outside of λ can be labeled naturally with monomials as in Figure 14. The ideal I_λ is then generated by these monomials. Thus, for $\lambda = (7,4,2,2,1)$ we get

$$I_\lambda = \langle x^7, x^4y, x^2y^2, xy^4, y^5\rangle.$$

It is easy to verify that the boxes inside λ correspond to monomials that constitute a $\mathbb{C}$-linear basis for the quotient $\mathbb{C}[x,y]/I_\lambda$. In particular, if λ is a partition of n then $\mathbb{C}[x,y]/I_\lambda$ has dimension n as a vector space over $\mathbb{C}$.

The torus $T = (\mathbb{C}^*)^2$ acts on H_n because it acts on $\mathbb{C}^2$ by scaling the axes. More concretely, if $I = \langle f_1(x,y), \ldots, f_r(x,y)\rangle$ is an ideal, then $(\sigma,\tau) \in T$ acts on I by

$$(\sigma,\tau)\cdot I = \langle f_1(\sigma x, \tau y), \ldots, f_r(\sigma x, \tau y)\rangle.$$

If $f(x,y)$ is a monomial, then $f(\sigma x, \tau y)$ is a scalar multiple of $f(x,y)$. Therefore, if all of the polynomials $f_i(x,y)$ are monomials, then $(\sigma,\tau)\cdot I = I$. In other words, if

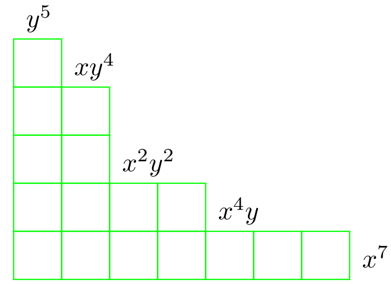

Figure 14. Monomials in the nooks immediately outside of the partition $\lambda = (7, 4, 2, 2, 1)$

$I = I_\lambda$ for some partition λ then I_λ is a T-fixed point of H_n. The converse holds as well: if I is a T-fixed point, then $I = I_\lambda$ is a monomial ideal for some partition λ.

For Hilbert schemes, therefore, combinatorics is evident already in the fixed points themselves, regardless of localization theorems. This makes fixed point formulas on H_n all the more interesting: any such formula will have a sum $\sum_\lambda \xi_\lambda$ over partitions λ of n on one side of the equation. What Haiman's geometric theory shows is that, for certain vector bundles and more general sheaves on H_n with interesting global section characters ξ, fixed point formulas result in extraodinarily interesting sums over λ.

The reason why the fixed point formulas are so interesting is that a certain particularly natural vector bundle on H_n yields summands ξ_λ that are essentially the *Macdonald polynomials* from Lecture 3 of Haiman's course. This statement is equivalent to the $n!$ theorem (see Theorem 8 in the notes by Haiman and Woo). One of the fixed point formulas it yields results in the $(n+1)^{n-1}$ theorem [**3**], a combinatorial statement that motivated the whole geometric story. It says that

$$R_n = \mathbb{C}[x_1, y_1, \ldots, x_n, y_n]/\langle x_1^r y_1^s + \cdots + x_n^r y_n^s \mid r, s \in \mathbb{N}\rangle,$$

which is known as the ring of *diagonal coinvariants*, has dimension $(n+1)^{n-1}$ as a vector space over $\mathbb{C}$. In fact, since the summands ξ_λ are torus-equivariant data at the fixed point I_λ, the fixed point formula is a doubly-graded version of this enumerative statement. Combinatorial methods for such *q, t-analogues* in general, and the Macdonald polynomials in particular, constitute Haiman's course.

8. Morse theory

Localization theorems are powerful ways to reconstruct topological invariants from knowledge of local data near fixed points. However, even to speak of fixed points we must have a group action. In the preceding situations, such actions were natural, in that they were fundamental to the smooth spaces under consideration. The flag manifold, for instance, is the quotient of a Lie group by a closed subgroup, and hence obviously has lots of Lie group actions on it; and a toric variety is (by some definitions) the closure of a dense torus orbit. But what if our smooth space doesn't come with a natural Lie group action? Make a group action from scratch!

Suppose that X is a real manifold with a Riemannian metric. Any real-valued function $f : X \to \mathbb{R}$ yields a *gradient flow* on X: each point goes in the direction of steepest descent. Gradient flow can be viewed as an action of the Lie group $\mathbb{R}$

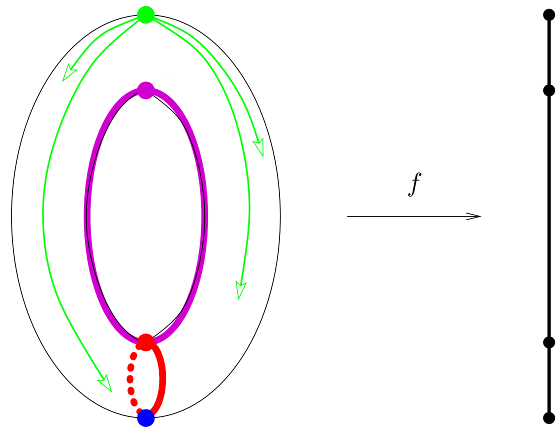

Figure 15. Four critical points on a torus, with the negative flow directions

(thought of as parametrizing time) on X. The fixed points of the flow are the critical points of f, where the derivative of f vanishes; these points are ambivalent about which direction to go, so they stay put. See Figure 15 for an example with four critical points on a torus. When f is generic, we can define the *index* of a critical point x to be the number of independent directions at x in which the flow points away from x—that is, the limit is x as time approaches $-\infty$.

Topological invariants are extracted from this (more or less) combinatorial data of critical points, indexes, and downward flow submanifolds by constructing a cell decomposition of X. There is one cell for each critical point, and the dimension of the cell is the index of the critical point. From Figure 15, we see that a torus can be constructed from a vertex (the bottom critical point), two edges (the middle two critical points), and one 2-cell (the top critical point). The manner in which the downward flow submanifold from one critical point approaches the other critical points determines how to glue the cells.

Gradient flow is all well and good if we're given a smooth manifold. But what if, in the spirit of how this Overview started, we're given a discrete geometric object, such as a collection of polytopes or a simplicial complex Δ? The answer lies in Forman's lectures: use discrete Morse theory. The idea is strikingly simple. Let P be the Hasse diagram of the face poset of Δ. Orient all of the edges of P downward. A *Morse flow* in this context is a (partial) matching on P such that reversing the edges in the matching does not ruin the directed acylicity property of the directed graph P. This mirrors the stipulation that our Morse function f mapped X to the real numbers, and not (for example) to the circle. The *critical simplices* of the Morse flow are the unmatched elements of P. In analogy with the smooth case, the critical simplices correspond to cells in a complex that is homotopy-equivalent to Δ, so the topological invariants have not changed. Discrete Morse theory is an extremely useful tool in making explicit calculations. It is also a key theoretical tool for poset homology, which leads to Wachs's course.

Going beyond Morse theory, it is possible to combinatorialize a number of other notions from differential geometry. Forman's fourth and fifth lectures, for example, discuss combinatorializations of curvature, and the purely combinatorial questions that result as a consequence. Of course, combinatorialization often helps us understand the smooth setting better. Recent work of Biss [**1**], for example, shows that understanding metric tangent data in a purely combinatorial context loses no topological information whatsoever. The discrete analogues of smooth tangent bundles are, in that case, matroid bundles on combinatorial differentiable manifolds ("CD-manifolds").

9. Further topics

We have tried in this Overview to give an idea of what "geometric combinatorics" might mean, although (for obvious reasons) we have done so mostly in the context of the courses at PCMI 2004. But this summer's offerings are by no means comprehensive! There are vast numbers of ways combinatorial structure arises in geometry. Here, for example, is a small list of keywords.

- Tropicalization: polyhedral structures reflect the geometry of complex algebraic varieties.
- Degeneration: replace a manifold or variety, such as a Schubert variety, by a degenerate version that has several components, each of which is simpler.
- Stratification: different strata, as in moduli spaces of curves, can represent collections of geometric objects with identical combinatorial properties.
- Branch point data (Hurwitz schemes and ramified covers): counting methods rely on combinatorics of the symmetric group.
- Generating functions: for example, Gromov–Witten theory leads to multivariate hypergeometric series.
- Characteristic classes: for example, functorial approaches to graph coloring and Tverberg-type theorems.

Some of the above items were hot topics at the 2004 PCMI Research Program: the Clay lecture by Sturmfels was one of many talks about tropical geometry and its applications, and the research talk by (for example) Vakil concerned recent advances using degeneration. The last item on the list was expanded by Kozlov to a survey paper that is included in this volume. The survey concerns *graph complexes* and functorial approaches to graph coloring. More precisely, in 1978 Lovász proved a subtle conjecture of Kneser in graph theory using functoriality: a proper vertex-coloring of a graph is intepreted as a morphism in a certain category of graphs. This leads to a morphism between two topological spaces with free $\mathbb{Z}_2$-actions, to which the Borsuk–Ulam theorem can be applied. Recently these techniques of graph complexes and characteristic classes have been greatly extended, culminating in Babson and Kozlov's proof of a conjecture of Lovász.

Keeping in mind that the above list is incomplete, it should be clear that there would never be enough time to cover all of the relevant topics. The only remedy would be another summer school on Geometric Combinatorics.

BIBLIOGRAPHY

1. D. K. Biss, *The homotopy type of the matroid Grassmannian*, Ann. of Math. (2) **158** (2003), no. 3, 929–952.
2. E. Freitag and R. Kiehl, *Étale cohomology and the Weil conjecture*, Ergebnisse der Mathematik und ihrer Grenzgebiete (3) [Results in Mathematics and Related Areas (3)] Vol. 13, Springer-Verlag, Berlin, 1988.
3. M. Haiman, *Vanishing theorems and character formulas for the Hilbert scheme of points in the plane*, Invent. Math. **149** (2002), 371-407.
4. M. Joswig and G.M. Ziegler, *Neighborly cubical polytopes*, Discrete Comput. Geom. **24** (2000), 325–344.
5. A. Okounkov and R. Pandharipande, *Gromov–Witten theory, Hurwitz numbers, and Matrix models, I*, preprint. arXiv:math.AG/0101147
6. G. Pick, *Geometrisches zur Zahlenlehre*, Sitzungsberichte Lotos (Prag), Natur-med. Verein für Böhmen **19** (1899), 311–319.